MAGNETICALLY ACTUATED RECONFIGURABLE PIXELATED ANTENNA

Jitendra Pal[1], Kaustubh Deshpande[1], Lou Chomas[1], Suresh Santhanam[1], Francesco Donzelli[2], Daniele Piazza[2], James A. Bain[1], and Gianluca Piazza[1]
[1]Carnegie Mellon University, Pittsburgh, USA
[2]Adant Technologies, Padova, ITALY

ABSTRACT

In this paper, a 6-element pixelated antenna with reconfigurable resonance frequency and polarization is presented. Reconfiguration is achieved by mechanically connecting/disconnecting 6 movable Ni patches to/from fixed Cu patches, hence realizing patch antennas of different sizes and shape. Each movable patch is a cantilevered plate, micro-fabricated from a Ni layer plated on an RT Duroid substrate. The Ni patch is magnetically actuated by means of an electro-permanent magnet (EPM) placed behind the ground plane of the antenna. Since the Ni patch is itself part of the radiating element, this approach eliminates the need to insert an external switch on the antenna plane. The EPM is placed behind the ground plane, therefore eliminating losses associated with bias lines generally used in pixelated antennas. Most importantly, the very low mechanical contact resistance (as low as 200 mΩ) between the Ni and Cu patch ensures high antenna efficiency. The EPM enables latching of the magnetic actuator, hence resulting in zero static configuration power consumption. Measured resonance frequency reconfigurability, radiation pattern and radiation efficiency agree well with simulated data.

INTRODUCTION

An efficient reconfigurable antenna is highly desirable for responding to the issue of spectrum scarcity. A significant amount of research has been conducted on reconfigurable antennas because of their ability to switch patterns, frequency and polarization using semiconductor or RF MEMS switches [1-5]. Compared with PIN diodes, MEMS switches offer higher linearity, lower insertion loss, and higher isolation [6-7]. However, semiconductor or MEMS switches have typically only been integrated within the antenna plane using wire bonding or soldering, in a hybrid integration topology. Such approaches suffer from significant losses, coming from either the switch itself or the presence of parasitics and bias lines. In [8] MEMS switches were monolithically integrated on the antenna to mitigate the issue associated with hybrid integration. However, these RF MEMS switches were actuated electrostatically, requiring via holes through the ground plane for bias lines connected to each switching element. These biasing lines introduce additional losses for the radiating element. Generally, a pixelated antenna requires a large number of switches, such that this approach will significantly affect antenna performances.

In order to actuate the switch without interrupting the ground plane with metallic lines, we use magnetic actuation, which can operate over larger distances than electrostatic transducers. We generate localized magnetic fields from below the ground plane under each switch by means of an array of electro-permanent magnets (EPMs). The use of EPMs removes the need for bias lines going through the ground plane. Furthermore, the use of EPMs enables the switch to latch into on and off states without static power consumption. Power is consumed only when the EPM needs to be switched in order to open or close the patch. Since the switch itself works as the radiating element, there is no need to insert external packages onto the antenna plane.

ANTENNA CONCEPT & FABRICATION

Figure 1 illustrates the schematic of a reconfigurable patch antenna microfabricated directly on an RT Duroid substrate with thickness of 381 µm, relative dielectric permittivity of 2.2, and loss tangent of 0.0004. In this first prototype, a total of 6 movable elements and four fixed patches all surrounding a central feed patch are used to demonstrate the basic capabilities of the proposed technology. Specifically, our goal is to show frequency and polarization reconfigurability. The movable patches are made of relatively magnetically soft nickel. The area of the each of the magnetic patch (Figure 2) is 2.5 x 2.5 mm^2 to ensure sufficient reconfiguration and tessellation. The anchor area was designed large enough to account for undercut from the release process, thereby minimizing the effect of stress gradients. FEM predicts the patch deflects approximately 20 µm for a stress gradient of 2 MPa/µm (see Figure 2).

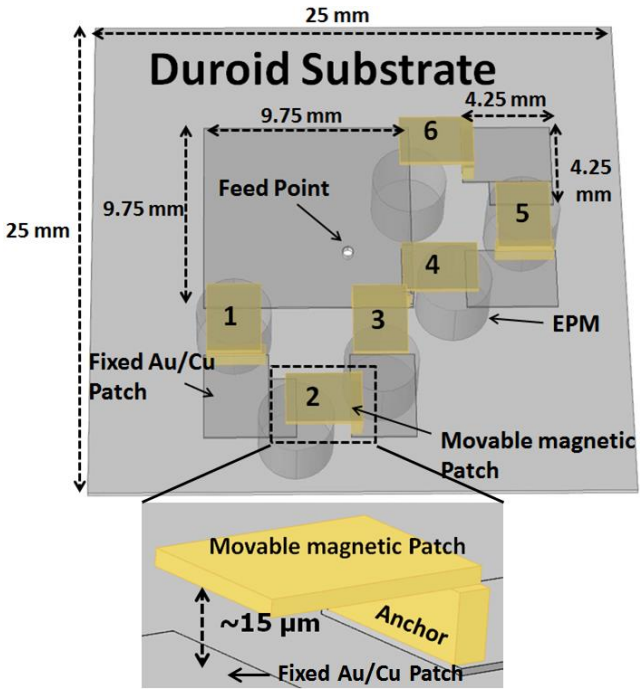

Figure 1: Schematic diagram of the 6-element antenna and zoomed in view of the movable patch

In order to get good electrical contact between nickel and the fixed patches, a thin layer of Au (500 nm) is deposited on top of 9 µm thick copper to form the fixed patches. The movable patch is actuated by a simple, but innovative EPM design. The EPM is formed by an AlNiCo5 rod wound with 200 turns of Cu wire as shown in Figure 3. To close the switch, a 100 µs current pulse is applied in a specific direction such that the EPM gets magnetized and pulls the patch towards the fixed Au-coated Cu patch forming a strong metallic contact. To open the switch, a current pulse in the reverse direction with a specific (reduced) magnitude demagnetizes the EPM. Consequently, in the reduced magnetic field, the Ni patch has sufficient restoring force to break the contact and open the connection with the fixed Cu patch.

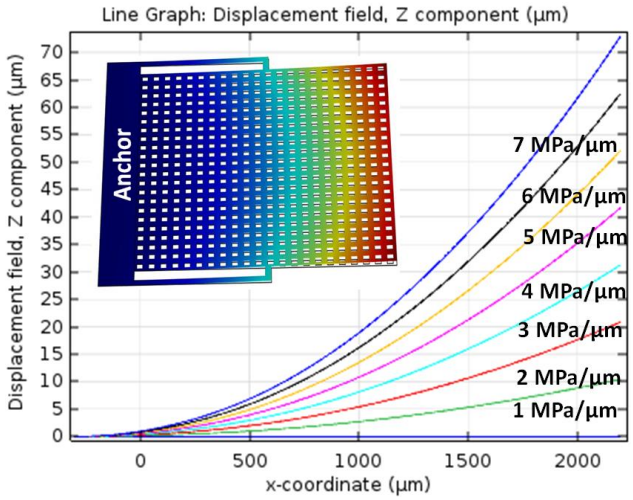

Figure 2: Calculated movable Ni patch displacement along the centerline for different stress gradient levels.

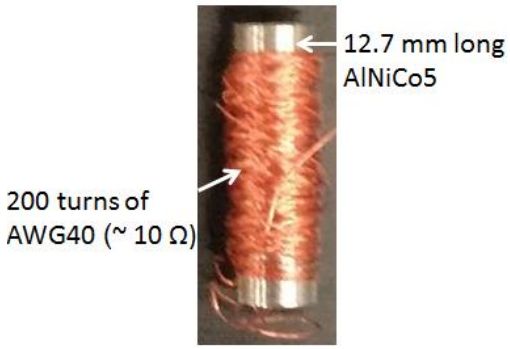

Figure 3: In-house developed EPM formed by winding (with AWG 40 wire) a 3.175 mm diameter AlNiCo5 rod (12.7 mm long)

Figure 4 shows the fabrication process flow for an antenna with 6 movable elements. First, a Cr (200 nm)/Au(500 nm) composite layer is patterned on the copper by photoresist patterning, sputtering and ion-milling, resulting in Figure 4a. A uniform seed layer of 1 µm sputtered Cu for the nickel plating of the switch is then deposited (Figure 4b). An 8 µm thick nickel layer is then electroplated using a patterned thick photoresist mold as shown (after mold removal) in Figure 4c. Finally, the device is released using wet etching (Figure 4d). To control the stress gradient and the curvature of the released cantilevers, the current density of the electroplating step was varied. Figures 5a and 5b show the relation between measured switch end deflection and the calculated stress gradient for different plating currents. In all experiments the temperature was kept constant at 54^0 C. By increasing the current density from 0.56 A/dm^2 to 1.69 A/dm^2, the average deflection at the end of the cantilever beam was decreased from 95 µm to 11 µm while the average (calculated) stress gradient was reduced from 5.8 MPa/µm to 0.65 MPa/µm (Figure 5b). As we increase the current density beyond 1.69 A/dm^2 the cantilevers exhibit an asymmetric stress gradient and in some cases touch the substrate. Figures 6 and 7 show images of the micro-fabricated 6-element antenna and an SEM micrograph of the fabricated Ni patch. This Ni patch was deflected approximately 15 µm for a current density of 1.69 A/dm^2, which corresponds to a stress gradient of approximately 1.6 MPa/µm.

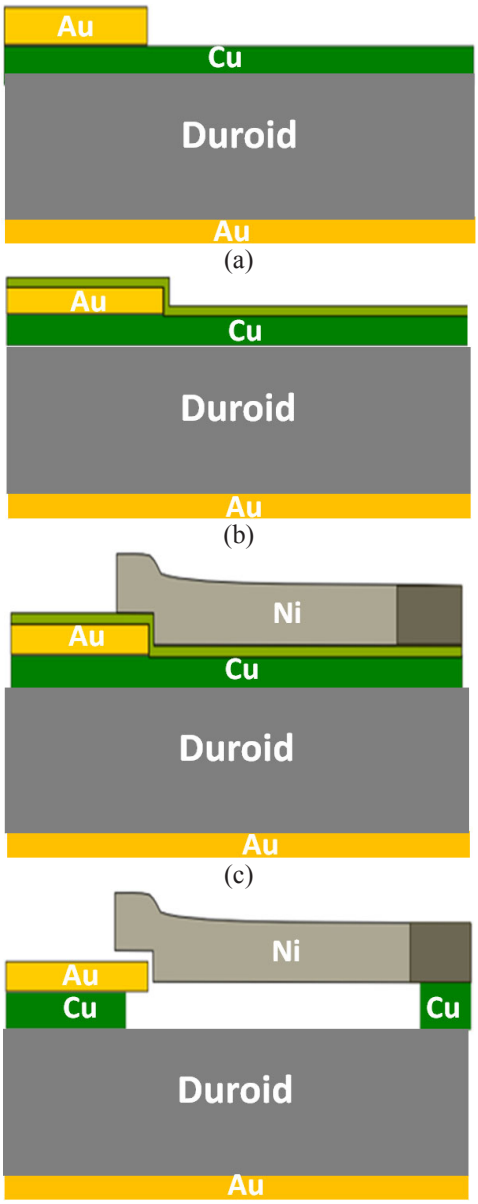

Figure 4: Fabrication process flow of the 6-element antenna: (a) sputter and pattern Au; (b) sputter Cu seed layer; (c) Ni plating; (d) Cu tech to release switch.

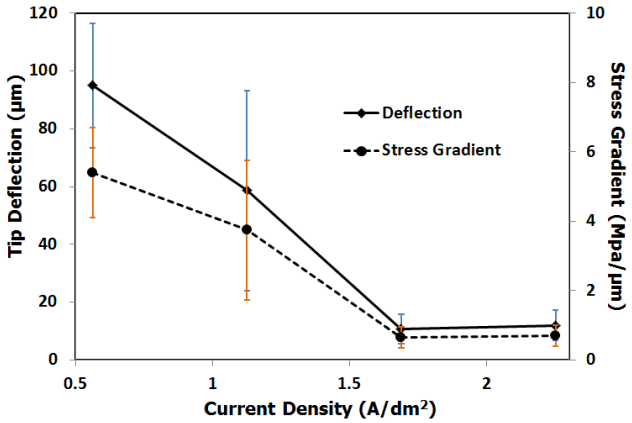

Figure 5: Ni patch deflection (end) (left axis) and calculated stress gradient (right axis) vs Ni plating current density. The error bars show the standard deviation of cantilever deflections and stress gradients across the wafer for each plating condition.

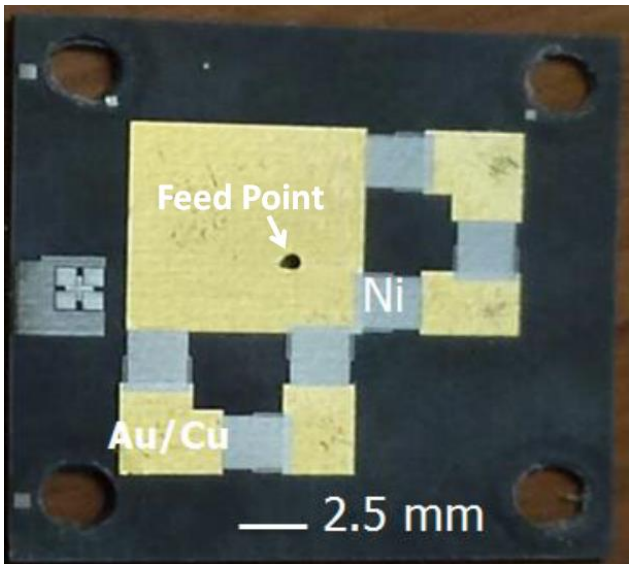

Figure 6: Image of the micro-fabricated 6-element antenna.

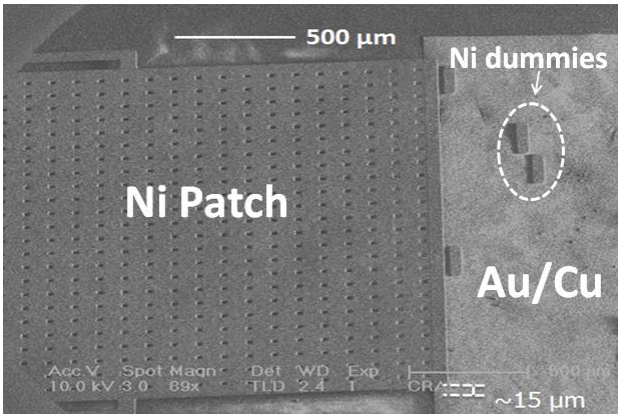

Figure 7: SEM micrograph of the fabricated patch. Ni dummies are included to ensure constant plating areal density is attained across wafer. The 4 rectangular elements remaining on the fixed patch are residues of the dummies that were plated throughout the Duroid to ensure a constant plating area for different mask sets.

EXPERIMENTAL RESULTS

The antenna prototype formed by 6 movable Ni patches has four significant RF configurations as shown in Figure 6, centered around the following frequencies: 8 GHz (ALL-OFF), 5.5 GHz (123-ON with vertical polarization), 5.5 GHz (456-ON horizontal polarization), and 6.5 GHz (ALL-ON).

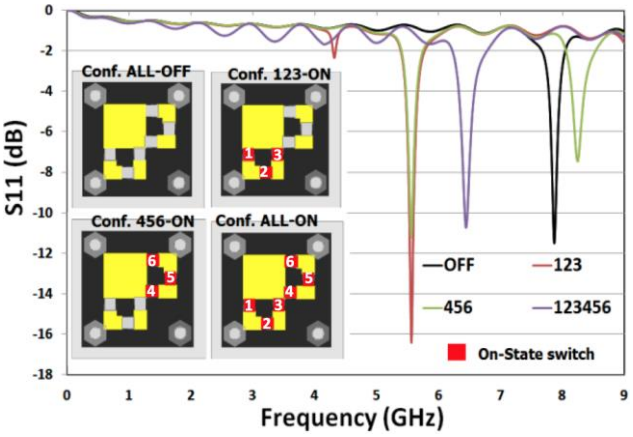

Figure 8: Measured voltage reflection coefficient (S11) of fabricated antenna in different configurations.

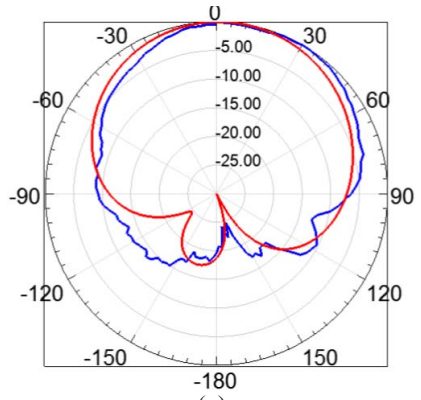

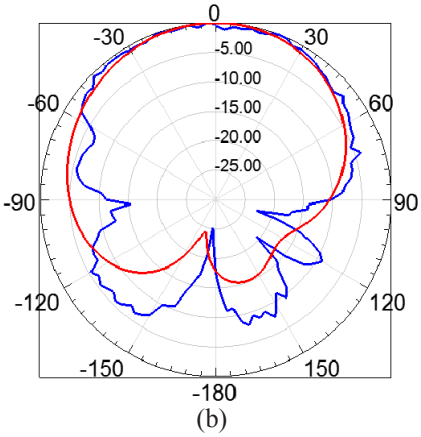

Figure 9: Normalized radiation patterns (in dB) of the 6-element antenna at 5.55 GHz (a) Conf. 123-ON vertical polarization, (b) Conf. 456-ON horizontal polarization. Plots are normalized to the maximum gain (3.5 dBi for Conf. 123-ON and 3.4 dBi for Conf. 456-ON).

The contact resistance for the fabricated Ni patches was measured using a four-point probe, with each patch having a contact resistance from 200 mΩ to 300 mΩ when actuated with the EPMs. A voltage of 70 V and a max current of ~ 7A are required to generate the maximum magnetic field in the EPM and toggle the switch to the ON position. A –30 V pulse is used to minimize the magnetic field out of the EPM (by demagnetizing it) and hence ensuring that the switch returns to the open position.

The reflection coefficient of the antenna (S11) was measured using Agilent 8722ES network analyzer after a one-port short-open-load (SOL) calibration. The radiation patterns and radiation efficiency were measured using an RFX2 EM scanner. Figures 8 and 9 illustrate the reflection coefficient, radiation pattern and peak gain measurement results for the fabricated antenna prototype. The measurements agree reasonably well with simulations. Most importantly, frequency and polarization configuration were demonstrated with this simple prototype. The antenna gain exhibited a value around 3.5 dBi at 5.55 GHz for configurations 123-ON and 456-ON, confirming that the Ni patches have a minimal impact on antenna radiation efficiency.

CONCLUSION

RF MEMS technology compatible with PCB technology has been used to create a monolithically integrated reconfigurable RF MEMS pixelated antenna system. RT Duroid was used because of its low dielectric constant and loss tangent. Reconfigurability is achieved by connecting/disconnecting movable Ni patches to fixed Cu patches. Since the Ni patch is actuated using a EPM situated below the ground plane, frequency and radiation patterns are not affected by the bias lines, which are generally used to drive any other switch technology. The proposed design uses a simple 3 mask process which can be made readily compatible with PCB fabrication processes. Measured and simulated results are in good agreement, validating the proposed concept.

ACKNOWLEDGEMENTS

The material is based upon work supported by the Defense Advanced Research Projects Agency (DARPA) under Contract No. HR0011-14-1-0056. Authors would like to thank the staff of Carnegie Mellon University's Nanofabrication facility for their kind and continuous support.

REFERENCES

[1] T. Aboufoul, A. Alomainy, and C. Parini, "Reconfiguring UWB Monopole Antenna for Cognitive Radio Applications Using GaAs FET Switches", *IEEE Antennas Wireless Propagation Letter*, vol. 11, pp. 392-394, 2012.

[2] D. Rodrigo, B. A. Cetiner, and L. Jofre, "Frequency, Radiation Pattern and Polarization Reconfigurable Antenna Using a Parasitic Pixel Layer", *IEEE Trans on Antennas and Propagation*, vol. 62, pp. 3422-3427, 2014.

[3] A. Mansoul, F. Ghanem, M. R. Hamid and M. Trabelsi, "A Selective Frequency-Reconfigurable Antenna for Cognitive Radio Applications", *IEEE Antennas Wireless Propagation Letter*, vol. 13, pp. 515-518, 2014.

[4] H. Rajagopalan, J. M. Kovit, and Y. Samii, "MEMS Reconfigurable Optimized E-Shaped Patch Antenna Design for Cognitive Radio", *IEEE Trans on Antennas and Propagation*, vol. 62, pp. 1056-1064, 2014.

[5] T. J. Jung, I. J. Hyeon, C. W. Baek, and S. Lim, "Circular/Linear Polarization Reconfigurable Antenna on Simplified RF-MEMS Packaging Platform in K-Band", *IEEE Trans on Antennas and Propagation*, vol. 60, pp. 5039-5045, 2012.

[6] P.G Grant and M.W. Denhoff, "A Comparison Between RF MEMS Switches and Semiconductor Switches", in *Proceedings of the 2004 International Conference on MEMS, NANO and Smart Systems*, Alberta, Aug 25-27, 2004, pp. 515-521.

[7] J. Pal, Y. Zhu, J. Lu, D. Dao, and F. Khan, "High Power and Reliable SPST/SP3T RF MEMS Switches for Wireless Applications", *IEEE Electron Device Letters*, vol. 37, pp. 1219-1222, 2016.

[8] A. G. Besoli, and F. D. Flaviis, "A Multifunctional Reconfigurable Pixeled Antenna Using MEMS Technology on Printed Circuit Board", *IEEE Trans on Antennas and Propagation*, vol. 59, pp. 4413-4423, 2011.

CONTACT

*Jitendra Pal; jpiitr84@gmail.com